Archives of Materials Science and Engineering

Volume 28
Issue 8
August 2007
Pages 453-460

International Scientific Journal
published monthly as the organ of
the Committee of Materials Science
of the Polish Academy of Sciences

Analysis of FSW welds made of aluminium alloy AW6082-T6

J. Adamowski [a,*], C. Gambaro [b], E. Lertora [b], M. Ponte [b], M. Szkodo [c]

[a] Global Service Engineering R&D, Ansaldo Energia, Via N. Lorenzi 8, 16152 Genoa, Italy
[b] Department of Production Engineering, Thermoenergetics and Mathematical Models, University of Genoa, Via All'Opera Pia 15, 16145 Genoa, Italy
[c] Faculty of Materials Engineering, Gdańsk University of Technology, ul. Narutowicza 11/12, 80-952 Gdansk, Poland
* Corresponding author: E-mail address: jaroslaw.adamowski@fastwebnet.it

Received 02.04.2007; published in revised form 01.08.2007

ABSTRACT

Purpose: of this paper is to analyze the results of tests on the mechanical properties and microstructural changes in Friction Stir Welds in the aluminium alloy 6082-T6 in function of varying process parameters.

Design/methodology/approach: : the produced tensile strength of the produced welds was measured and the correlation with process parameter was assessed. The welds' microstructure in various zones was analyzed using an optical microscope. Microhardness measurements were performed on the welds' cross-sections.

Findings: a tendency was observed of the mechanical resistance of test welds to increased with the increase of travel (welding) speed, maintaining constant rotational speed. Hardness decrease was observed in weld nugget and heat affected zone, of entity inferior that that of fusion welds. Origins of tunnel (worm hole) defects were found and analyzed.

Research limitations/implications: various combinations pf process parameters were used to produce the test welds, but without the possibility of controlling the downward force. Further extension of applicable parameters combinations should be examined.

Practical implications: the increase of mechanical resistance with increasing welding speed offers an immediate economic return, as the process efficiency is increased.

Originality/value: information contained herein can be useful to further investigate on the possibility of improving the properties of FSW welds, as well as the efficiency of the process.

Keywords: Welding; FSW; Aluminum alloys

MATERIALS MANUFACTURING AND PROCESSING

1. Introduction

In many industrial applications steels are readily replaced by non-ferrous alloys, in most cases by aluminium alloys. Some of these materials combine mechanical strength comparable with structural steels and low weight, allowing for a significant reduction of weight. While production of components of aluminium alloys is not very complex, joining of these materials can sometimes cause serious problems [1]. Lack of structural transformations in solid state and excellent thermal and electrical conductivity cause problems in fusion and resistance welding of aluminium alloys [2]. That led to the development of Friction Stir Welding [3] a solid state joining technique in which the joined material is plasticized by heat generated by friction between the surface of the plates and the contact surface of a special tool, composed of two main parts: shoulder and pin [4]. Shoulder is responsible for the generation of heat and for containing the plasticized material in the weld zone, while pin mixes the material of the components to be welded, thus creating a joint (Fig.1). This

allows for producing defect-free welds characterized by good mechanical and corrosion properties [17-19]. This paper summarizes the results of an experimental campaign in which the aluminium alloy AW6082-T6 was FSWelded, using various combinations of process parameters (rotational and travel speed). Mechanical properties of the test welds were assessed by means of static tensile test, bending test. Macro and microstructure of the welds were examined by means of optical observations and Vickers hardness measurement.

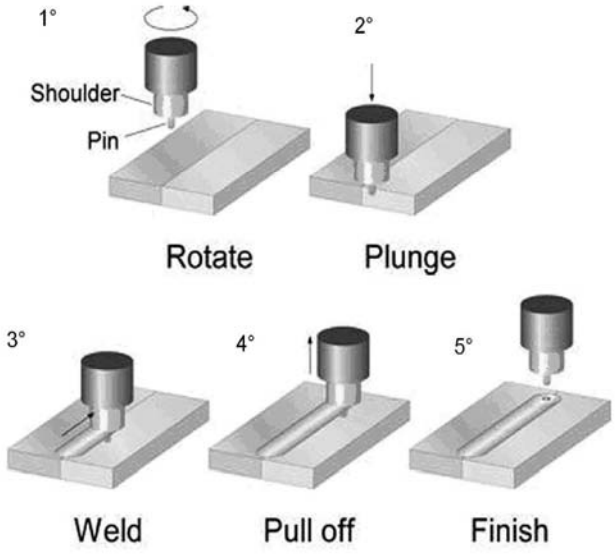

Fig. 1. Schematic representation of FSW process

2. Experimental

2.1. Production of joints

The experiments were conducted on the aluminium alloy AW-6082-T6, its chemical composition and principal mechanical properties are respectively presented in tables 1 and 2. Given the Al-Mg-Si alloys are rather easily weldable even with conventional techniques, it was decided to verify weldability of the chosen alloy by the widest possible range of parameters.

Table 1.
Chemical composition of AW-6082 (EN 573-3)

Si	Fe	Cu	Mn	Mg	Cr	Zn	Ti
0.70 1.30	0.50	0.10	0.40 1.00	0.60 1.20	0.25	0.20	0.10

Table 2.
Mechanical properties of AW-6082-T6 (EN 485-2)

Tensile strength [MPa]	Yield strength [MPa]	A_5 [%]	HB
≥310	≥260	10	94

The work station used to produce welds was a converted milling machine [5]. The parameters (rotational and travel speed) chosen for welding are presented in table 3. Welds were made of laminated plates having the following dimensions: 300x150x5mm. The material of the welding tool was a structural steel of resistance class 8.8. The diameter of the shoulder was 19mm, while the pin was a M6 bolt. The length of the pin was set at 4.8mm, which was slightly less than the thickness of welded plates. In case of all welds a 20 second preheat time was applied in order to increase the plasticity of the material and decrease the bending loads on the pin.

The temperature of the welded plates was monitored during welding with thermocouples placed on both sides of the joint line, 15 mm from the weld axis. The thermocouples N°. 1, 2 and 3 were located on the advancing side of the weld respectively at the distance of 80mm, 110mm and 140mm from the weld starting point. The thermocouples No. 4, 5 and 6 were placed on the advancing side of the weld, at the same longitudinal distribution.

Table 3.
FSW welding parameters for AW-6082-T6 alloy

Weld number	Rotation [rpm]	Travel [mm/min]	Weld number	Rotation [rpm]	Travel [mm/min]
FSW-01	230	115	FSW-07	880	170
FSW-22	330	115	FSW-13	880	260
FSW-21	330	170	FSW-14	880	390
FSW-04	460	115	FSW-15	880	585
FSW-09	460	170	FSW-03	1230	115
FSW-19	460	260	FSW-06	1230	170
FSW-05	630	115	FSW-10	1230	260
FSW-08	630	170	FSW-11	1230	390
FSW-17	630	260	FSW-12	1230	585
FSW-20	630	390	FSW-16	1700	390
FSW-02	880	115	FSW-18	1700	585

2.2. Examination of joints

All welded samples were visually inspected in order to verify the presence of possible macroscopic external defects, such as surface irregularities, excessive flash, and lack of penetration or surface-open tunnels.

Temperature measurements revealed a significant difference between the advancing and retreating side of the welds.

Tensile tests were performed on samples cut perpendicularly to the weld line. The tests were carried out at constant speed of 5mm/min.

X-ray examination was also carried out to verify the presence of possible volumetric defects in the test welds.

Microhardness of the welds was measured with the test load of 200g. The indentations were made at midsection of the thickness of the plates across the joint.

Mechanical properties of the test welds were assessed by means of tensile tests and 3-point bend test. The ultimate tensile

stress (UTS) value was measured in the tensile test and the bend angle was measured in the bend test.

Metallographic specimens were cut mechanically from the welds, embedded in resin and mechanically ground and polished using abrasive disks and cloths with water suspension of diamond particles. The chemical etchant was the Keller's reagent. The microstructures were observed on optical microscope.

3. Discussion of results

3.1. Temperature acquisition and visual inspection

The temperature on advancing sides of weld was higher than on retreating side. The average temperature difference of 50°C was noticed. This difference is a result of an asymmetry of the FSW process [6,7]: total linear velocity of the perimeter of the shoulder is higher on the advancing side than on the retreating side. Figure 2 represents the temperature diagram acquired during the execution of weld FSW-02.

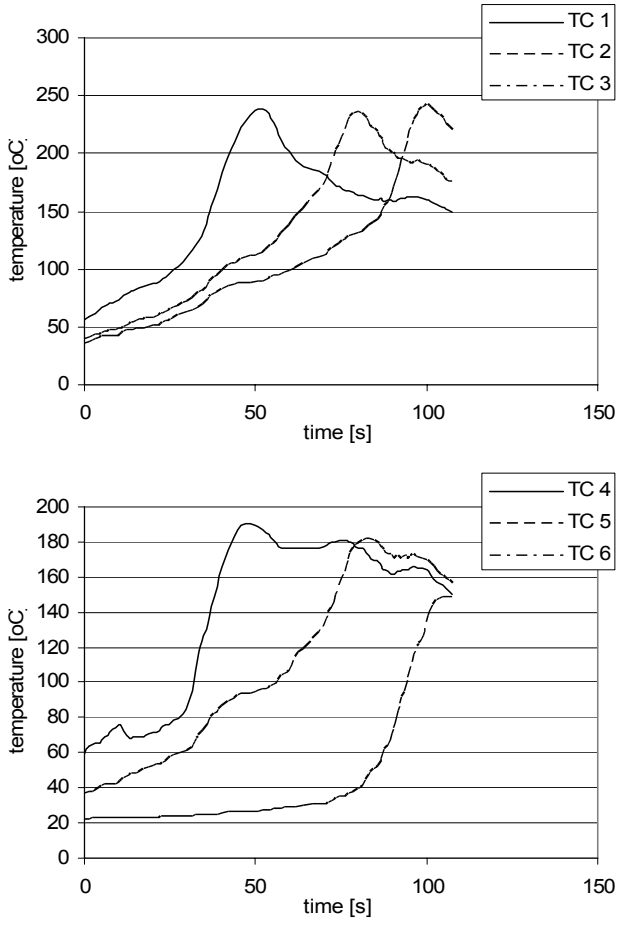

Fig. 2. Temperatures acquired in the weld FSW-02

The diagram in figure 3 represents a relation between the process parameters and the maximum temperature generated during welding. As the transverse (welding) speed increases and at constant rotational speed of the tool, the heat input tends to decrease. This phenomenon results in a decrease of the temperature to which welded elements are heated. The greatest temperature values measured during the experimental campaign reached c.a. 250°C (FSW-05).

Taking in consideration the following factors:

- location of the thermocouples in respect to the weld axis – at the distance of 15mm from the weld line,
- a relatively high thickness of the welded elements,
- excellent thermal conductivity of aluminium,

It is obvious that a rather big temperature gradient can be expected. From that it can be deduced that the temperatures at the weld center can reach values even twice as high, close to 500°C.

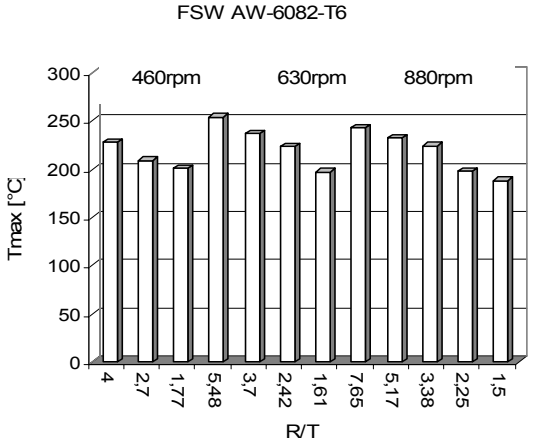

Fig. 3. Maximum temperature as a function of R/T ratio

3.2. Visual inspection

During visual inspection several types of defects were revealed. Excessive lateral flash was also observed in most of the welds, resulting from the outflow of the plasticized material from underneath of the shoulder (Fig. 4).

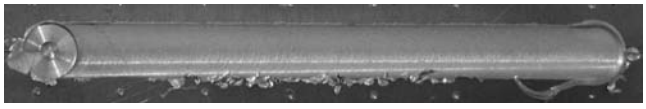

Fig. 4. Lateral flash in the joint FSW-18

In case of the joint FSW-06 a surface-open tunnel was found (fig.5) as a result of insufficient downward pressure [8].

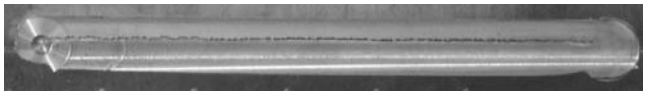

Fig. 5. Surface open tunnel in weld FSW-06

A comparison between two welds produced using the same travel speed of 115mm/min and with different rotational speeds is presented in figure 6.

It can be seen that in case of the "hotter" weld (1230rpm and 115mm/min) it has a rough surface covered with particles of aluminium giving an abrasive paper-like appearance. Such poor surface quality is attributable to the fact that at high temperatures generated during welding, the particles of aluminium tend to attach themselves to the surface of the shoulder of the tool and are plucked out of the weld face surface and transferred to another location. Local liquation melting cannot also be excluded.

The other, "colder" weld has a smooth, regular surface. The values of rotation-to-travel speed ratio (R/T) for the below presented welds were 10,7 and 4, respectively for "hot" and "cold" weld.

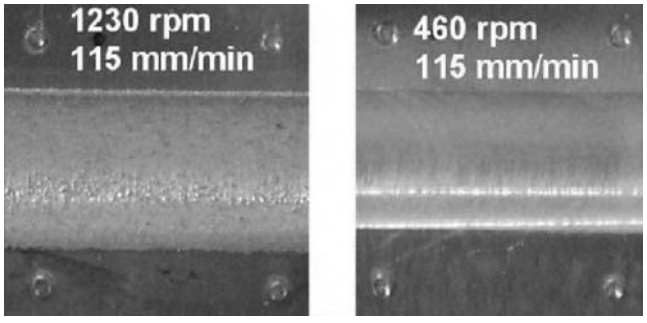

Fig. 6. Surface quality of "hot" and "cold" welds

3.3. X-ray tests

All test welds were examined by the X-ray method, except for the sample FSW-06, in which the surface open tunnel was present. Most of the joints were sound; only in some cases two subsurface defect types were observed:

- Tunnel in the initial part of the joint (fig.7). This type of defects is caused by the insufficient plasticization of the welded material for the applied travel speed. Such condition can take place over the distance of c.a. 50-70mm (thermal transition zone) until the process reaches its thermodynamic equilibrium – a situation in which the travel (welding) speed is approximately equal to the velocity of propagation of the heat wave in the welded material.
- Tunnel running along the entire length of the weld – In his case the thermodynamic equilibrium condition was not reached (fig. 8).

In the radiographs below can also be seen the outflows of the plasticized material, surface irregularities and weld face concavity, that can correlated to the tool axis' inclination angle.

Fig. 7. Internal tunnel defect in the initial part of weld FSW-12

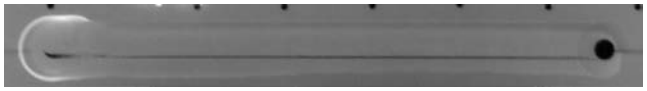

Fig. 8. Internal tunnel defect in weld FSW-6

3.4. Tensile tests

In all cases the samples failed in HAZ of the advancing side, similarly as reported in [9]. The results are presented in Fig.9a and 9b. It can be noticed that at constant rotational speed mechanical resistance of joints increases with increasing of the travel speed. This can be attributed to the decreased heat input and relative limited softening of the material in HAZ.

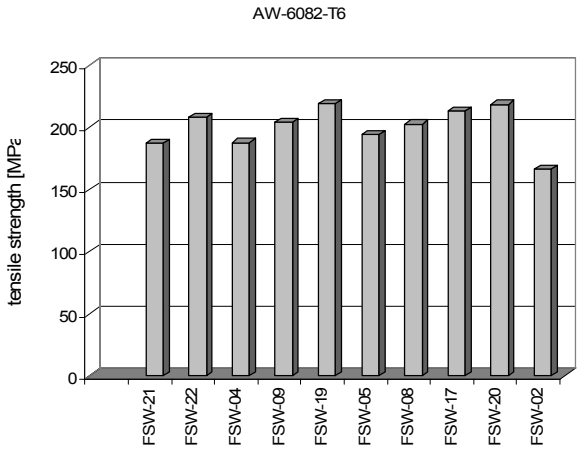

Fig. 9a. Results of tensile tests

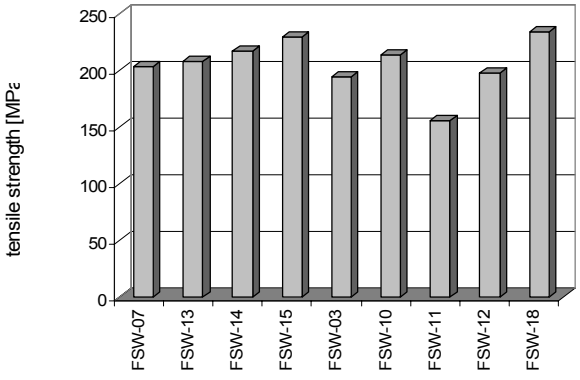

Fig. 9b. Results of tensile tests

3.5. Bend tests

Bend tests were performed on both face and root side of the welds. Most of the welds presented good ductility, allowing for very high bend angles. Such ductility is a well known characteristic of the 6082 alloy, and in case of FSW technology it

has been preserved, thanks to the lower heat input (than that of fusion welding methods) and the dynamic recrystallization of the weld nugget microstructure. In case of weld samples that broke during the bend tests, the reason behind it is an incorrect mixing of the material and insufficient downward force. Both of these are attributable to the lack of tool's force and/or position feed-back system, which would have guaranteed the stability of the set process parameters during the realization of the welds. The delamination fracture mentioned in table 4, along with a sound sample are presented in figure 10.

Fig.10. Bend samples

Table 4.
Results of the bend test

Bend angle (average of 2 samples)					
Weld	FSW	FSW	FSW	FSW	FSW
number	02-02	02-03	02-04	02-05	02-07
Face	180°	180°	180°	180°	180°
Root	180°	180°	180°	180°	180°
Weld	FSW	FSW	FSW	FSW	FSW
number	02-08	02-09	02-10	02-11	02-12
Face	180°	180°	180°	75°	70°
Root	180°	180°	180°	180°	180°
Weld	FSW	FSW	FSW	FSW	FSW
number	02-13	02-14	02-15	02-16	02-17
Face	180°	Delamination	180°	5°	180°
Root	180°	180°	90°	5°	180°
Weld	FSW	FSW	FSW	FSW	FSW
number	02-18	02-19	02-20	02-21	02-22
Face	20°	180°	Delamination	180°	180°
Root	15°	180°	180°	170°	180°

3.6. Microhardness measurements

Figure 11 represents the hardness diagram of the joint FSW-10. The hardness of both the heat affected zone (HAZ) and the weld nugget (WN) is lower than that of base metal (BM), respectively by 15-20% and 7-10%. The difference between HAZ and WN is attributable to the grain refinement in WN, caused by intensive stirring. The softest points of the joints correspond to the failure locations in tensile tests.

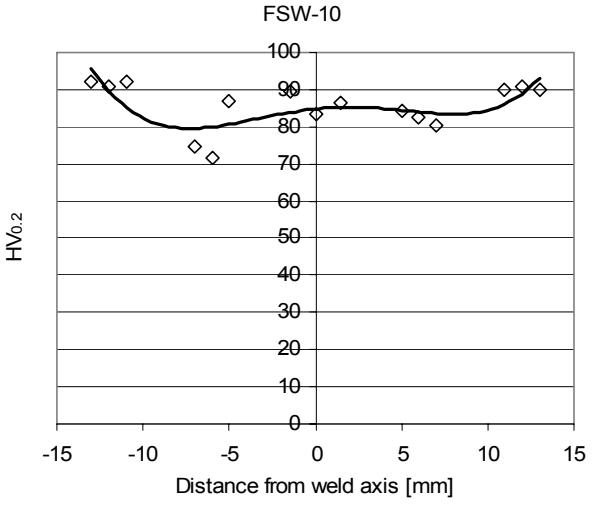

Fig. 11. Hardness profile of the weld FSW-10

3.7. Microstructural evaluation

Microstructures of various zones of FSW joints, in particular case of the joint FSW-03 are presented in figure 12. The base material contains elongated grains with average dimensions LxH equal to 100x30 μm. In weld nugget the grains are much smaller and equiaxed of average diameter 1-5μm. This grain refinement is a result of dynamic recrystallization [10,11,12], i.e. a combined action of high rate strain and elevated temperatures. Such recrystallized structure is characterized by a very low level of residual stresses, excellent ductility and mechanical properties superior to those of heat affected zone [13].

The concentric rings visible in weld nugget, are called "onion rings" and are a typical feature of FSW process. Their presence documents the complex mechanics of the process: a combination of rotational, longitudinal and vertical movement of the plasticized material [14,15]. This structure is a result of the tool pin's mixing and forging action and is strictly related with the R-T ratio. At constant rotational speed the distance between bands located at the same distance from weld centre increases with increasing the travel speed, hence with decreasing the R-T ratio.

The weld nugget is a part of a bigger zone, the Thermo-mechanically Affected Zone (TMAZ), in which grains are deformed: elongated and rotated due to the strain to which they were subjected during welding. Moving away in the direction of base material, the following zone is heat affected zone (HAZ).

There the microstructure is similar to that of base material, only the grains are slightly overgrown as a result of the exposure to welding heat.

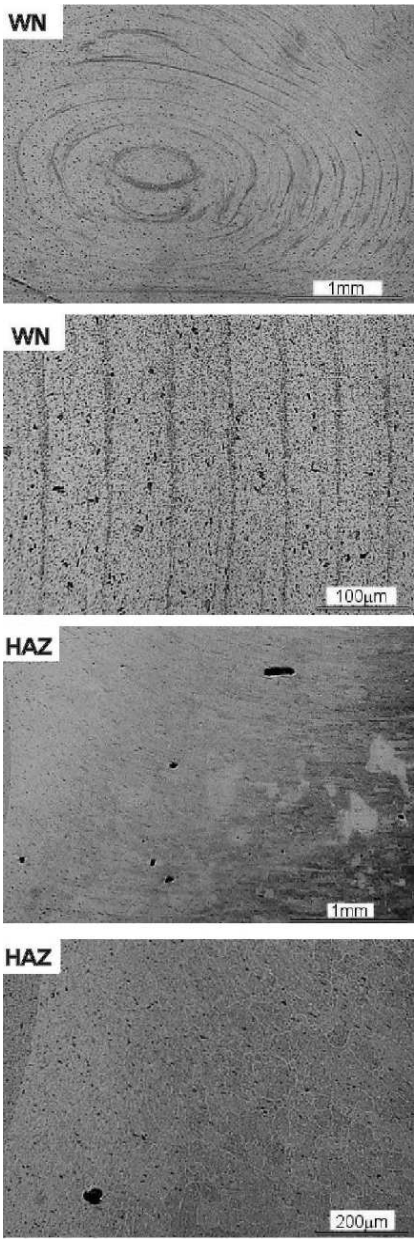

Fig. 12. Microstructures in various zones of the weld FSW-03

An interesting artifact was found in the sample FSW-03 (Fig. 13). At the intersection of weld nugget, thermo mechanically affected zone and flow arm (a band of material running from WN towards the joint surface border on advancing side) the three distinct zones are starting to separate, giving origin to a tunnel defect. These defects are attributable to the combination of parameters: either insufficient or excessive rotational speed combined with too low downward force. In such case the welded parts cannot be correctly stirred and mixed together and a tunnel (also called "worm hole") is created, running along the entire weld [16,20,21]. The abovementioned flow arm is presented in figure 14.

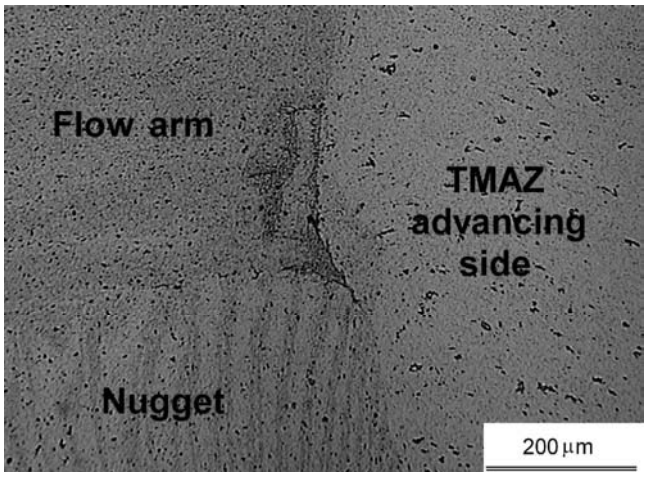

Fig. 13. Initial stage of tunnel defect in the weld FSW-03

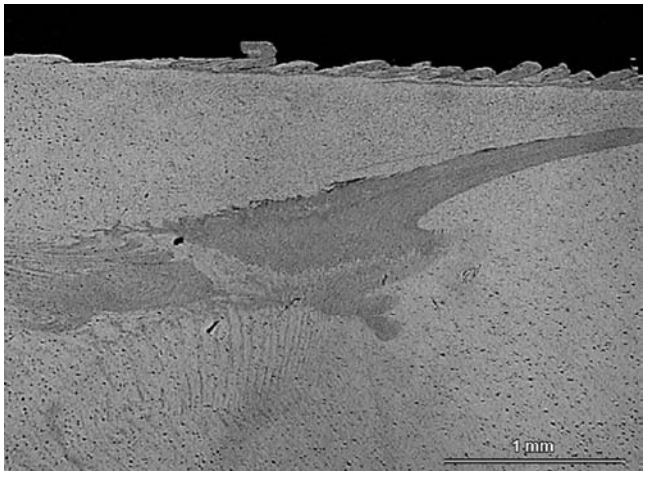

Fig. 14. Flow arm in a FSW weld

Such situation in which the tunnel is beginning to form, but there is no actual metal separation, must be considered rather dangerous since it is difficult to detect with conventional non destructive test methods, especially when they are performed at construction site and not in laboratory conditions. The X-ray exam did not reveal that defect, as this test method is based on the difference of absorption of radiation by parts of examined material characterized by different density and orientation, i.e. when there is an inclusion of different material or a clear separation of material preferably in the direction parallel to the direction of radiation. The ultrasonic exam could be more reliable in revealing such defects since it is based on the reflection of acoustic waves from any obstacles. A problem with ultrasonic exam on aluminium is related to a rather coarse grained microstructure of aluminium. In such case long grain boundaries act as interface lines for the acoustic wave and the resulting signal is characterized by very intense noise,

making it almost impossible to identify possible to distinguish noise from defects.

3.8. Range of welding parameters

The results of the destructive and non-destructive tests aimed at assessing the quality of FSW welds allow to graphically represent the weldability of the AA6082-T6 alloy by FSW in form of a weldability chart (fig.15). Apparently better results are obtained when using relatively low rotational and travel speeds. A sound, defect-free weld was, however, also produced with rotational speed of 1700rpm and travel speed of 585mm/min. The FSW workstation used in the experiments didn't allow for tests using rotational speed values above 1700rpm, which could be extremely interesting from the economic yield point of view. If an assumption is made that the travel (welding) speed is in strict relation with the rotational speed then increasing the rotational speed above the examined 1700rpm would allow for increased welding rate. Several additional benefits could result from it:

- no increase of the consequent heat input if the rotational to travel speed ratio is maintained,
- ultra fine grained structure in the weld nugget due to more intense mechanical action of the tool's probe on the plasticized material,
- improved dynamic recrystallization mechanism due to higher strain rate at approximately constant temperature,
- improved flow of the plasticized material and hence the material's distribution across the welds section.

One thing must be kept in mind when consulting parameter selection charts for the Friction Stir Welding process. Unlike in case of fusion welding, here the parameters are optimized for a given tool geometry, with particular stress on the diameter of the shoulder. If the same parameters are applied with a tool having smaller shoulder, sufficient temperature of the welded material may not be obtained and it may be impossible to produce sound welds.

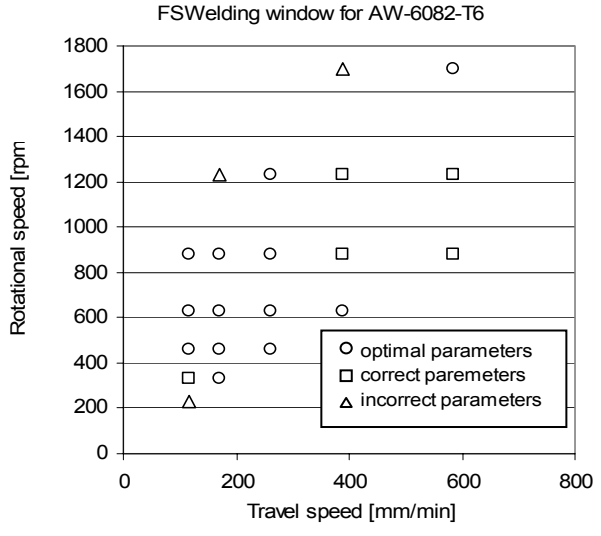

Fig. 15. FSWelding parameters chart for AW-6082-T6

Similarly the form of the pin should be taken into consideration. Smooth, non-threaded, conical or cylindrical pins usually limit the applicable parameters range as they do not guarantee adequate stirring especially in case of insufficiently plasticized material. Introducing threaded, swirl, or flute features on the pins allows for a better, more efficient mixing of the plasticized material and, as a result obtaining a joint characterized by a more homogeneous structure, as well as superior mechanical properties.

4. Conclusions

Mechanical properties of Friction Stir welded aluminium alloy 6082-T6 exhibit a variation with changing of process parameters. Tensile strength of FSW welds is directly proportional to travel (welding) speed. Softening of the material was observed in the weld region. This softening was most evident in the heat affected zone on the advancing side of the welds and corresponded to the failure location in tensile tests. The reason for this phenomenon was the kinetic and thermal asymmetry of the FSW process. An initial stage of a longitudinal, volumetric defect was found at the intersection of weld nugget and thermo-mechanically affected zone. Friction Stir Weldability for Aw-6082-T6 alloy chart was created.

Acknowledgements

The authors would like to express their gratitude towards the Italian Institute of Welding, Genoa, Italy, for allowing to use their laboratory equipment during the preparation and analysis of the welds.

References

[1] A.K. Jha, S.V.S.N. Murty, V. Diwakar, K. Sree Kumar, Metallurgical analysis of cracking in weldment of propellant tank, Engineering Failure Analysis 10 (2003) 265-273.

[2] G. Huang, S. Kouc, Partially melted zone in aluminum welds - liquation mechanism and directional solidification, Welding Research Supplement, 2000, 113-120.

[3] W.M. Thomas, E.D. Nicholas, J.C. Needham, M.G. Murch, P. Templesmith, C.J. Dawes, International Patent application N° PCT/GB92/02203, 1993.

[4] T. Dickerson, Q. Shi, H.R. Shercliff, Heat flow into friction stir welding tools, Proceedings of the 4th International Symposium on Friction Stir Welding, Park City, Utah, USA, 2003.

[5] M. Ponte, J. Adamowski, C. Gambaro, E. Lertora, Low cost transformation of a conventional milling machine into a simple FSW work station, Advanced Manufacturing Systems and Technology 4 (2005) 357-365.

[6] A. Simar, T. Pardoen, B. de Meester, Influence of friction stir welding parameters on the power input and temperature distribution in aluminum alloys, Proceeding of the 5th International FSW Symposium, Metz, France, 2004.

[7] P. Heurtier, M.J. Jones, C. Desrayaud, J.H. Driver, F. Montheillet, D. Allehaux, Mechanical and thermal

modelling of Friction Stir Welding, Journal of Materials Processing Technology 171 (2006) 348-357.
[8] Y.G. Kim, H. Fujii, T. Tsumura, T. Komazaki, K. Nakata, Three defect types in friction stir welding of aluminum die casting alloy, Materials Science and Engineering A 415 (2006) 250-254.
[9] H.J. Liu, H. Fujii, M. Maeda, K. Nogi, Tensile properties and fracture locations of friction-stir-welded joints of 2017-T351 aluminum alloy, Journal of Materials Processing Technology 142 (2003) 692-696.
[10] J-Q. Sua, T.W. Nelson, C.J. Sterling, Microstructure evolution during FSW/FSP of high strength aluminum alloys, Materials Science and Engineering A 405 (2005) 277-286.
[11] A. Barcellona, G. Buffa, L. Fratini, D. Palmeri, On microstructural phenomena occurring in friction stir welding of aluminum alloys, Journal of Materials Processing Technology 177 (2006) 340-343.
[12] J. Ouyang, E. Yarrapareddy, R. Kovacevic, Microstructural evolution in the friction stir welded 6061 aluminum alloy (T6-temper condition) to copper, Journal of Materials Processing Technology 172 (2006) 110-122.
[13] H.G. Salem, Friction stir weld evolution of dynamically recrystallized AA2095 weldments, Scripta Materialia 49 (2003) 1103-1110.
[14] K.N. Krishnan, On the formation of onion rings in friction stir welds, Materials Science and Engineering A327 (2002) 246-251.
[15] J. Yan, M.A. Sutton, A.P. Reynolds, Process-structure-property relationship for nugget and HAZ region of AA2524-T351 FSW joints, Proceeding of the 5th International FSW Symposium, Metz, France, 2004.
[16] P. Cavaliere, G. Campanile, F. Panella , A. Squillace, Effect of welding parameters on mechanical and microstructural properties of AA6056 joints produced by Friction Stir Welding, Journal of Materials Processing Technology 180 (2006) 263-270.
[17] T. Watanabe, H. Takayama, A. Yanagisawa, Joining of aluminum alloy to steel by friction stir welding, Journal of Materials Processing Technology 178 (2006) 342-349.
[18] A. Squillace, A. De Fenzo, G. Giorleo, F. Bellucci, A comparison between FSW and TIG welding techniques: modifications of microstructure and pitting corrosion resistance in AA 2024-T3 butt joints, Journal of Materials Processing Technology 152 (2004) 97-105.
[19] M. Czechowski, Low-cycle fatigue of friction stir welded Al–Mg alloys, Journal of Materials Processing Technology 164-165 (2005) 1001-1006.
[20] J. Adamowski, C. Gambaro, M. Ponte, E. Lertora, Investigation on Friction Stir Welding weldability of the aluminium alloy AA6082-T6, 7mo Convegno AITeM, Lecce, Italy, 2005.
[21] J. Adamowski, M. Szkodo, FSW of aluminum alloy AW6082-T6, Journal of Achievements in Materials and Manufacturing Engineering 20 (2007) 403-406.